Study the evaluation of underactuated robotic gripper

Cite as: AIP Conference Proceedings **2395**, 050010 (2021); https://doi.org/10.1063/5.0068177
Published Online: 18 October 2021

K. Ganesh, Ajith Arul Daniel, R. Pugazhenthi, et al.

Study the Evaluation of Underactuated Robotic Gripper

K. Ganesh[1], Ajith Arul Daniel[2], R. Pugazhenthi[2,a] and P. Balamurali[3]

[1]*Mai-Nefhi College of Engineering and Technology, Eritrea*
[2]*Department of Mechanical Engineering, Vels Institute of Science, Technology & Advanced Studies, Chennai, India*
[3]*Department of Mechanical Engineering, Chennai Institute of Technology, Chennai - 600069, India*

[a]*Corresponding author: pugal4@gmail.com*

Abstract. In this paper, a newly developed underactuated gripper robotic gripper is designed and fabricated and is tested and simulated by the optimal force. This kind of robot gripper can adapt the grasped object depending on shape and output grasping force. This model has created a linkage-based parallelogram mechanism to include kinematic and contact constraints. Geometric optimization of three phalanges underactuated fingers is presented based on a Finite Element analysis technique. Multi-objective optimization is used for evaluating finger parameters that were associated with link position, grasping equilibrium, and contact force. All optimal parameters of the mathematical models are obtained by using Ansys software. In order to test the optimum force of the finger, a wide range of contact positions was selected, and found exact position different grasping shapes. In this experiment, the grasping force is measured and compared with numerical results. The results obtained by both simulation and experiments exhibit a good correlation with the analytical results.

Key words: Underactuated finger, Finger with force augmentation, Robotic finger, Gripper

INTRODUCTION

The increasing research interest in the field of robot end effectors particularly grippers is growing worldwide and is beyond the boundary of applications. Grippers are easily controlled and thereby it obtains large grasping force as output [1, 2]. A good underactuated gripper must have a shape adaptability character. Aaron M Dollar and Robert D Howe [3] introduced joint coupling configuration of the gripper in underactuated robotic grippers for unstructured environments that the object properties and location may not be known. This configuration gives maximum grasp range and minimum contact forces for a wide range of target object sizes and positions [4].

A better shape adaptation increases the number of contact points between the gripper and the object [5]. Increasing the number of contact points provide a better repartition of contact forces, which ensures better stability of grasp and prevents deterioration of the grasped object. However, their grasping dexterity and compliance are limited. In contrast, when designing and evaluating the contact forces of the gripper are minimized in order to avoid damaging the object [6, 7]. An underactuated mechanism has fewer actuators than degrees of freedom. This underactuated robot hand requires a large grasping force and a simple control mechanism.

The developed underactuated finger is required adaptive control that the object to be grasped automatically and adapted its conditions according to the object shape without complex control strategies [8]. Lionel Birglen and Clement M. Gosselin [9] designed three phalanx underactuated fingers with transmission mechanisms based on tendons and pulleys grasp stability with fewer degrees of freedom. This mechanism adjusts itself to an irregularly shaped object without a complex control strategy [10-12].

LITERATURE REVIEW

Many researchers have investigated the designing method for maximizing the contact, optimal synthesis technique in kinematics, force transmission capability, and analysis of the singularity configuration of the

Recent Trends in Manufacturing Technologies, Materials Processing, and Testing
AIP Conf. Proc. 2395, 050010-1–050010-8; https://doi.org/10.1063/5.0068177
Published by AIP Publishing. 978-0-7354-4141-5/$30.00

parallelogram mechanisms. A large range of external forces or torques is required to apply to the mechanical system of under-actuation. They are often vital constraints for feasible motions of a gripper. A few alternatives allow to complementing the control scheme in order to overcome the constraints. Auxiliary parallelogram mechanism to the fingers is a solution to obtain stable precision grasps. However, such an auxiliary mechanism complicates the design and makes it expensive.

Hoyul Lee et al introduced a simple triggered element in one of the joints of the fingers which can also keep the distal phalanges initially parallel [13]. Such a joint is normally locked by a spring and a mechanical limit releases when contact with the object and the proximal phalanx is encountered. The predominant advantages of the parallel mechanisms have higher structural stiffness and larger load-carrying capability with specific position accuracy than those of the serial one. However, the parallel mechanisms have disadvantages such as smaller workspace, lower dexterity and more complication in kinematics and dynamics, and difficulty of motion control in the large range of manipulation space.

Most of the researchers have attempted to describe the relationship between the input torque of the finger and the output contact forces on the phalanges [14]. The conventional analytical methods are a very challenging task for calculating desired grasping force. A recent advance in the field of adaptive grasping is the adoption of the principle of under-actuation. These grippers are capable to grasp a large range of objects, while their number of actuators and sensors remains limited. Fuzzy logic, Finite Element Analysis, and Neural Network-based systems are considered as potential for such an application. Dalibor Petkovic et al [15] developed an adaptive neuro-fuzzy network to make a model between contact point locations and contact forces. The input of the fuzzy controller was the contact force error, while its output was the actuator torque variation by considering the position error which is defined as the difference between the reference setpoint and the current joint angle. Actuator force is continuously given until the required contact force is attained. These contact forces are highly sensitive functions of the joint angles of the finger and contact locations on the phalanges [16].

From the above discussion, it can be understood that each type of grippers has its advantages and disadvantages. The research explores the improvement of the grasping ability without increasing the space and power required and can control complexity by incorporating the benefits of an underactuated finger into a gripper.

DESIGN OF THE UNDER-ACTUATED ROBOTIC GRIPPER

The three-fingered under-actuated robotic hand is developed for the unstructured environment. The finger of the gripper is composed of three phalanxes which consist of proximal, middle, and distal phalanxes. A macro size finger model is fabricated for experimentation. The line diagram of the finger is shown in Fig.1. This finger is driven by a hydraulic actuator and the drive input force is calculated. In this setup, three contact force sensors are mounted to measure the contact forces of each phalanx. These sensors are interfaced with a computer. In this underactuated gripper, the applied force is transmitted to the phalanges through four-bar mechanical linkages and springs.

The finger mechanism is composed of two four-bar linkages connected in series and the distal phalanx at the end. In which the first link a1 is the input link to one of the 4-bar mechanisms and the output is taken from all three-contact links. The input force is given by a hydraulic cylinder to the first four-bar linkage from the transmission mechanism that will move the first phalanx of the finger then moves the second four-bar linkage that will move the second phalanx and finally the third phalanx which represents the output links of the second four-bar linkage. The three links are formed to three different angular positions of the gripper to grasp the object.

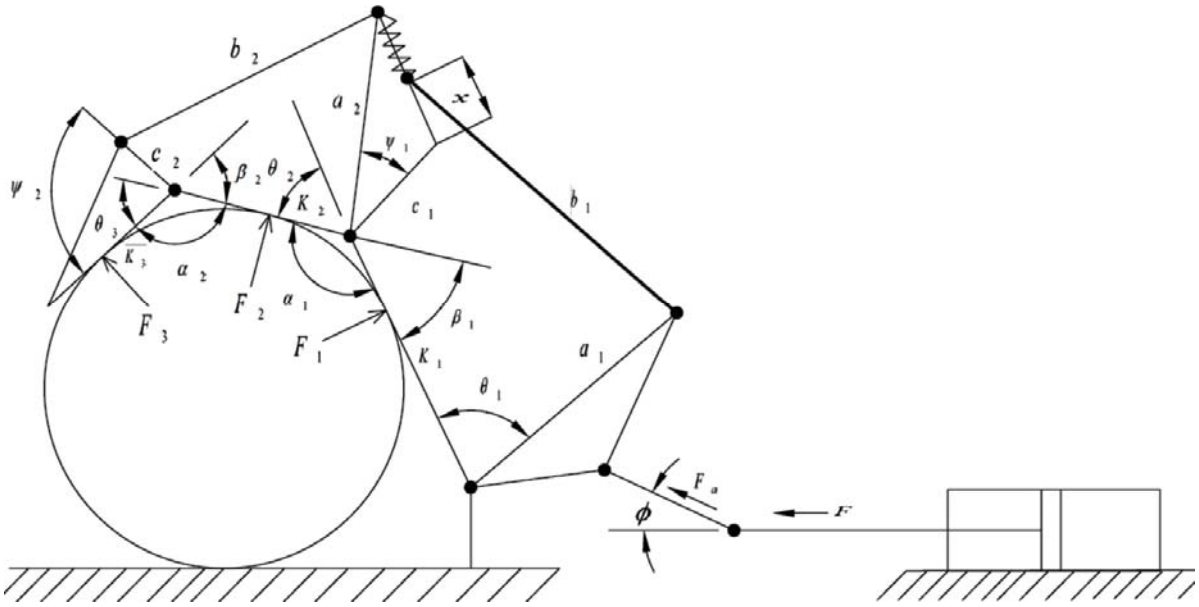

FIGURE 1. Geometry of the underactuated finger with a force augmentation

Fig.1 shows the dimensions, arrangements, and position of the links of the grippers. l1, l2, and l3 have represented the first, second, and third phalanx lengths respectively. k1, k2, and k3 have denoted the contact lengths of the first, second, and third phalanx which are to be optimized. θ1, θ2 and θ3 represent the angles of rotation of the first, second and third phalanges respectively with respect to the above said links and the 200 mm diameter of the object is maintained.As shown in Fig.1, there is a spring connected in the link1 and sliding along link2. The force exerted by spring can be decomposed parallel and perpendicular to the link. Spring is used for keeping the finger from its motion, but it still opposes the actuator force. However, sufficient stiffness is applied to keep the finger from collapsing. The application of a parallelogram mechanism to the fingers is a common solution to obtain stable precision grasps. Contact force sensors are used to acquire contact force information. This sensor feedback information greatly enhances the grasping stability and reduces the probability of mistakes in contact.

Grasping Force

The grasping force is calculated by contact forces in the gripper. The three phalanges of grippers are formed as shown in Fig.1. The position and orientation of the links with respect to the reference frame are given in this diagram. The contact lengths of the links are denoted as k_1, k_2,andk_3 respectively. The analytical expression of the contact forces F_1, F_2, and F_3 have been established in a static position. The contact forces are assumed to be normal and frictionless. Total contact force can be computed using a static analysis at each contact position for the grasping process. The static balance at each joint and the torque required to drive the phalanx can be calculated from the following:

$$T_3 = F_3 K_3 \tag{1}$$

$$F_3 = \frac{T_3}{K_3} \tag{2}$$

$$sin\beta_1 = \frac{a_1 - c_1}{l_1}$$

$$cos\beta_1 = \frac{b_1}{l_1}$$

$$T_2 = F_2K_2 - F_3l_2cos\alpha_2 + \frac{sxa_2c_1sin\psi_1}{c_{12}} \quad (3)$$

$$F_2 = \left(\frac{T_2}{K_2}\right) - \left(\frac{T_3l_2cos\alpha_2}{K_1K_3}\right) + \frac{sxa_2c_1sin\psi_{12}}{K_2c_{12}} \quad (4)$$

$$sin\beta_2 = \frac{a_2 - c_2}{l_2}$$

$$cos\beta_2 = \frac{b_2}{l_2}$$

$$T_1 = F_1K_1 + F_2l_1cos\alpha_1 + F_3(l_1 - l_2cos\alpha_2) + sx[c_{12} - l_1sin\psi_{23}] \quad (5)$$

$$F_1 = \left(\frac{T_1}{l_1 - l_2cos\alpha_2}\right) - \left(\frac{F_1K_1}{l_1 - l_2cos\alpha_2}\right) + \left(\frac{F_2l_1cos\alpha_1}{l_1 - l_2cos\alpha_2}\right) + \frac{sx[c_{12} - l_1sin\psi_{23}]}{l_1 - l_2cos\alpha_2} \quad (6)$$

where,

s- spring stiffness in N-m
x- displacement of the spring in m

The above equation is derived for finding contact forces on all phalanxes for a given actuating input force at static equilibrium. The mechanism of links are designed in such a way that is capable of only producing positive force at its contact points for the stability of the grasp. Similarly, the force required to drive the first phalanx can be calculated from the following:

$$F_a = Fcos\phi \quad (7)$$

$$F = pA$$

Where,

F –applied hydraulic force
ϕ – input link inclined with horizontal
A – piston area

The applied input force is maintained at 94.5961 N. This input force of 94.5961 N is sufficient to exert a grasping force. The magnitude and direction of the resolving applied force to each linkage varies depending on the link angles of θ_1, θ_2 *and* θ_3. The contact force expression is derived from a static analysis. Here our aim is to maximize the number of contacts between the fingers and the object and the total contact force for the grasping process. A contact force at each phalanx is assumed to be a pure force normal to the phalanx.

By varying the values of θ_1, θ_2, *and* $\theta_3$from $0^o$to $90^o$to obtain the maximum contact force between the phalanxes with the object to be grasped. Then, these variables are input into the GA to find the optimum contact force for the contact points. The objective of the gripper design is to minimize the actuation force and maximize the grasping force.

The fitness function represents an important part of the evolutionary process using Finite Element Analysis. Appropriate selection of the fitness function will lead the search towards the optimal solution. The optimal is to maximize the number of contacts between the fingers and the object and the total contact force for the grasping process. So, the fitness function is responsible for finding optimal results. The Finite Element analysis is planned to render an optimal contact force with maximum total contact force. The fitness functions 'f' is adapted for evaluating the optimal contact force which is defined as,

$$f_1 = T_2\left(K_1K_2 + K_1K_3cos\alpha_1cos\alpha_2 - \frac{T_3(K_1K_2cos\alpha_2)}{K_2cos\alpha_1 + (K_2 + K_3cos^2\alpha_2)}\right) \quad (8)$$

$$f_2 = T_2\left(K_1K_2 + K_1K_3cos\alpha_1cos\alpha_2 - \frac{T_3(K_1K_2cos\alpha_2)}{K_2cos\alpha_1+(K_2+K_3cos^2\alpha_2)}\right) \quad (9)$$

The index f_1 and $f_2$represent the maximum of total torque and total contact force where, k_1, k_2,andk_3 are the contact positions of three links.

TABLE 1 Geometric parameters of the linkages

l_1 mm	l_2 mm	l_3 mm	a_1 mm	b_1 mm	c_1 mm	a_2 mm	b_2 mm	c_2 mm	a_{11} mm	a_{12} mm	a_{22} mm	b_3 mm
155	100	95	120	145	70	125	160	40	75	70	80	100

Table 1 shows the geometric parameters of the linkages chosen for our gripper design. Using GA for the above geometric parameters optimum torque is found from iterative results as shown in Fig. 2 and the graph is drawn for actuating torque (Y-axis) Vs the Number of iterations (X-axis).

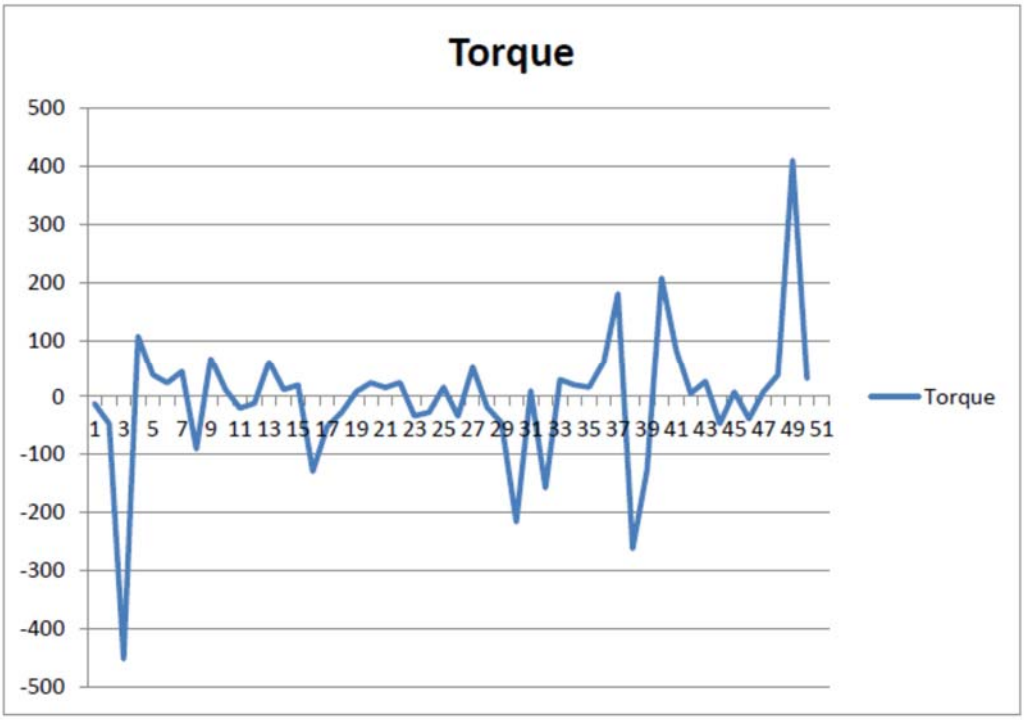

FIGURE 2. Optimum input torque obtained and its iterations

The optimum torque resulting from the iterations is Ta = 10.6426 N-m (at the end of 12th iteration) At this iterative point, the contact points and the phalanx angles are, k_1 = 66.54632 mm, k_2= 82.91371 mm, k_3 = 91.77619 mm, α_1 =152.46° and α_2 = 139.75°.

EXPERIMENTAL SETUP

In this experiment shown in Fig.3, the object that can be successfully made contact with this gripper and the contact force is measured. In order to test the optimum force of the gripper, a wide range of contact positions were selected, and found the exact position. It is very important and necessary to measure these contact forces in every phalange. The contact sensors are pasted into the phalanges plane to measure the contact force. The sensors are interfaced with Labview software for measuring contact force. The hydraulic actuator is used to drive the fingers and to make contact to acquire grasping force.

FIGURE 3. Robotic Gripper fabricated Model

In this experiment, the grasping force is measured five times and tabulated in the Table 2. The maximum grasping force is 81.8671N on average. This contact force on the object is compared with the optimum force. It can be inferred whether the grasping is adequate or not based on force information.

Table 2 Contact forces obtained from the contact sensors of the links

Sl.No.	Contact force F1 in N	Contact force F2 in N	Contact force F3 in N	Spring force Fs in N	Total contact force F in N
1	27.5924	24.9673	27.5924	1.715	81.8671
2	24.9673	22.2923	26.8315	1.715	75.8061
3	27.9673	23.1621	25.6758	1.715	78.5202
4	27.7566	24.8110	26.7566	1.715	81.0392
5	29.5917	22.6480	26.5917	1.715	80.5464
		Average			79.5558

From Table 2, the average total contact force is 79.5558N

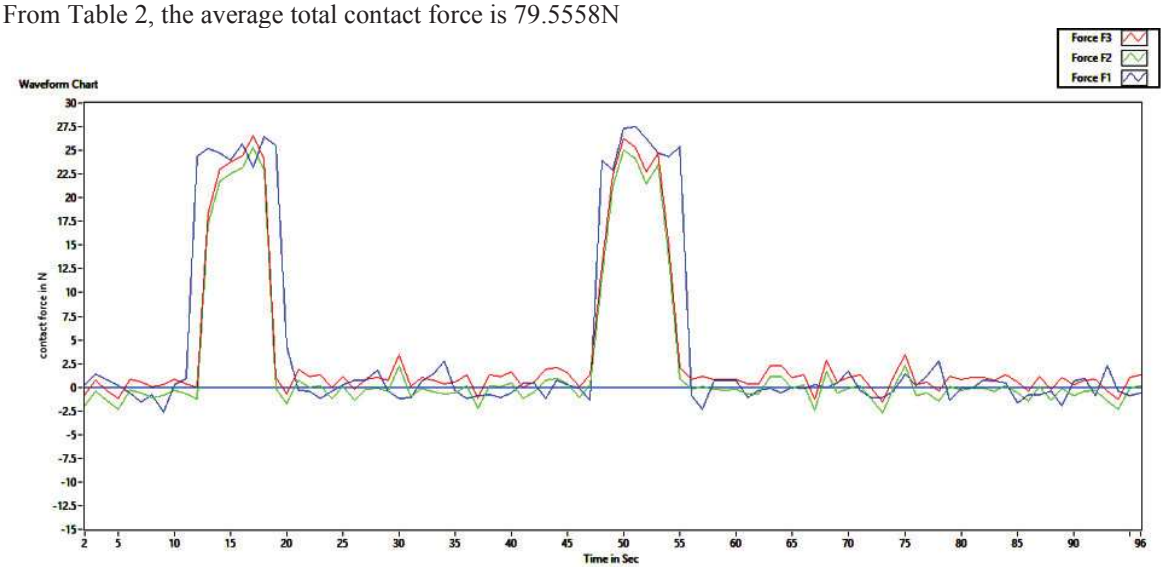

FIGURE 4. Measured contact forces

RESULTS AND DISCUSSION

It can be introduced that the maximize function of total contact force and the operating range of each link is usually limited by design parameters such as link lengths and fixed angles. The total magnitude of the contact forces on the objects grasped is relative to the actuation force which is also evaluated utilizing experimentation. From the results, it is inferred that how mechanical design is varied by these grippers dimensions and the distribution of the actuation force to the phalanges affects the performance. The optimum results show that the design parameters have a large influence on the behavior of the gripper. However, this mechanism is simple to determine the effect of each single design parameter it has on the behavior of the gripper. For these above reasons, it is made to develop experiments for calculating the permissible operating range according to Finite Element analysis design parameters. To verify the optimal force results, the total contact forces of the sensors are measured and compared with the results obtained by using equation (6). Figure. 4 shows the contact forces obtained from the contact sensors. The resulting force is calculated by summing three forces that are obtained from sensors. The resulting force is equal to the actuation force that is applied by the actuator. When the resulting force is zero, the force equilibrium at initial contact is not possible.

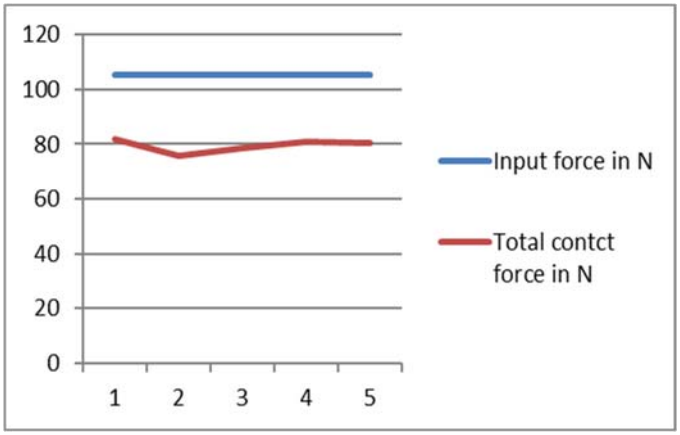

FIGURE 5. Relation of the input force and the total contact force

From the results, as shown in Fig.5, a conclusion can be drawn that when the finger is closed, the relation of the input force and the contact force on the object is approximated to linearity. According to the force information, the grasping force of each link is linearly varied because of its link contact positions.

The slider motion is resisting by the springs. Spring is used to avoid deteriorating the thrust force of this mechanism. The experimental results are shown in Table1, considering the spring force, the total contact force obtained is 79.5558N. Only 2.16% of the difference of contact force is obtained with and without spring. Since this difference is relatively small; it should be acceptable to have spring in the mechanism with a minimum spring constant that is enough to release the mechanism. From Table 2, the forces obtained by using GA and calculated from experimental data are approximately the same. In addition, the measured forces are in good correlation with the calculated forces. The deviation percentages range from 14.93% to 21.34%, which were possibly caused by errors in the fabrication of the link mechanism. During the grasping of the object, the proximal phalanx of the finger consistently maintained a slightly higher contact force than the other two phalanxes likely due to more contact action. The other contact force data is determined continuously staring one after other.

CONCLUSION

The different underactuated mechanisms are studied and obtained the optimum contact force for the designed underactuated gripper. This optimal design can only improve the performance of the mechanism and good grasping ability. Finite Element Analysis is used to find out the optimal contact force and other link parameters for increasing the quality of grasping. From the simulation results, the values of total contact force is 79.5558N and the contact position parameters k1, k2, and k3 are optimized at 66.54632mm, k2 = 82.91371 mm, k3 = 91.77619 mm respectively.The calculated optimum result of contact force is verified by experiments on a gripper and described.

The relation of the input force and the contact force on the object is found approximately linear. The calculated results of contact force are verified by experiments that strongly influence grasp performance. The results obtained through both simulation and experiments exhibit a good correlation with the analytical results.

REFERENCES

1. Shahram HadianJazi , Mehdi Keshmiri and Farid Sheikholeslam, Advanced Robotics, **22**, 1559-1584 (2008).
2. Antonio Bicchi and Vijay Kumar, Robotic grasping and contact: A review, IEEE international conference on robotics and automation, **1**, 348-353, March 2000.
3. Aaron M. Dollar; Robert D. Howe, Joint coupling design of underactuated grippers, Proc. ASME. 42568; **2**, 30th Annual Mechanisms and Robotics Conference, Parts A and B, 903-911, January 01, 2006.
4. Yoshikawa.T and Nagai.K, IEEE Transactions on Robotics, **7**(1), 67-77 (2002).
5. B. Barkat, S. Zeghloul, and J. P. Gazeau, Robotics and Autonomous Systems, **57**(4), 460–468 (2009).
6. Garg S, Dutta A. Inter. J. Adv. Robotic Systems, **3**(2), 107-114 (2006).
7. Wolniakowski K. Miatliuk · Z. Gosiewski · L. Bodenhagen, Journal Intelligent Robot Systems, **87**(1) 15-42 (2017).
8. Sarac M, Solazzi M, Sotgiu E, Bergamasco M, Frisoli A, Meccanica. **52**(3), 749-761 (2017).
9. Lionel Birglen and Clement M. Gosselin, J. Mech. Des **128**(2), 356-364 (2005).
10. Shaker S.Hasan, Somer M. Nacy, Eldaw E. Eldukhri, Haider Galil Kamil and Enass H. Flaieh, Control theory and informatics, **5**(3), 2015.
11. Stefan A.J. Spanjer , Ravi Balasubramanian, Aaron M. Dollar and Just L.Herder, ASME/IEEE International conferenece on reconfigurable mechanisms and robots, Tianjin, China, 669-679 (2012).
12. Clark, Angus B., Lois Liow, and Nicolas Rojas. J. Mech. Des. **143**(10), 104502 (2021).
13. Hoyul Lee, Youngjin Choi, and Byung-Ju Yi, IEEE/ASME Transactions on Mechatronics, **17**(1), 157-166 2012.
14. Birglen L, Gosselin CM, IEEE Transactions on Robotics and Automation. **20**(2), 211-221 (2004).
15. Wang, Daoming, et al. Mechanism and Machine Theory **155**, 104092 (2021).
16. Lee, Kiju, Yanzhou Wang, and Chuanqi Zheng. IEEE Transactions on Robotics, **36**(2), 488-500 (2020).